Journal of Molecular Graphics and Modelling 38 (2012) 148–154

Contents lists available at SciVerse ScienceDirect

Journal of Molecular Graphics and Modelling

journal homepage: www.elsevier.com/locate/JMGM

Binding pattern of the long acting neuraminidase inhibitor laninamivir towards influenza A subtypes H5N1 and pandemic H1N1

Arthitaya Meeprasert[a,1], Wasinee Khuntawee[b,1], Kittiwat Kamlungsua[a], Nadtanet Nunthaboot[c], Thanyada Rungrotmongkol[d,*], Supot Hannongbua[a,e]

[a] Computational Chemistry Unit Cell, Department of Chemistry, Faculty of Science, Chulalongkorn University, 254 Phayathai Road, Patumwan, Bangkok 10330, Thailand
[b] Nanoscience and Technology Program, Graduate School, Chulalongkorn University, 254 Phayathai Road, Bangkok 10330, Thailand
[c] Department of Chemistry, Faculty of Science, Mahasarakham University, Khamriang, Kantarawichai, Mahasarakham 44150, Thailand
[d] Department of Biochemistry, Faculty of Science, Chulalongkorn University, 254 Phayathai Road, Bangkok 10330, Thailand
[e] The Center of Excellence for Petroleum, Petrochemicals and Advanced Materials, Chulalongkorn University, 254 Phayathai Road, Patumwan, Bangkok 10330, Thailand

ARTICLE INFO

Article history:
Accepted 22 June 2012
Available online 4 July 2012

Keywords:
Laninamivir
Neuraminidase
H5N1
Pandemic H1N1
Molecular dynamics simulation

ABSTRACT

Influenza A H5N1 and pH1N1 viruses have broadly emerged and become widespread in various countries around the world. Oseltamivir, the most commonly used antiviral drug against the seasonal and pandemic influenza viruses, is targeted at the viral neuraminidase (NA), but some isolates of this virus have become highly resistant to this drug. The novel long-acting drug, laninamivir, was recently developed to inhibit influenza A and B viruses of either the wild-type (WT) or the oseltamivir resistant mutant of NA. To understand the high efficiency of laninamivir, all-atom molecular dynamics simulations were performed on the WT and H274Y mutant of H5N1 and pH1N1 NAs with laninamivir bound. As a result, the novel drug was found to directly interact with 11 binding residues mainly through salt bridge and hydrogen bond formation (as also seen by electrostatic contribution). These are comprised of 7 of the catalytic residues (R118, D151, R152, R224, E276, R292 and R371), and 4 of the framework residues (E119, W178, E227 and E277). Laninamivir showed a similar binding pattern to all four NAs, but strong hydrogen bonding interactions were only found in the WT strain, with a slightly lowered contribution at some drug contact residues being observed in the H274Y mutation. This is in good agreement with the experimental data that the H274Y mutant has a small increase (1.3–7.5-fold, which was not statistically significant) in the IC_{50} value of laninamivir.

1. Introduction

The avian flu (H5N1) and 2009 pandemic H1N1 (pH1N1) viruses are wide spread throughout the world and some isolates have become resistant to oseltamivir, the most common and (formerly) effective anti-influenza drug [1,2] (Fig. 1), leading to a potentially global public health problem. A new drug, laninamivir (R-125498), was approved and marketed in Japan in September 2010 [3]. With a long term inhibitory efficiency against the neuraminidase (NA) enzyme of influenza A and B viruses as well as their current oseltamivir resistant mutations [3–5], laninamivir is thus a very interesting drug not only for good efficacy but also in terms of a stockpile for future pandemic influenza. Although, the three dimensional structures of laninamivir binding to the wild-type (WT) NA subtypes N1 (from pH1N1, Fig. 2), N2 and N5 have recently been crystallized [6], the drug orientation and binding patterns towards the H5N1 virus and the H274Y (N2 numbering) mutant of both the pH1N1 and H5N1 viruses are not yet revealed. Therefore, the main goal of this present study was to provide a detailed comparative understanding of the drug–target interactions of laninamivir binding to the NA of both the WT and the H274Y mutant of these two N1 virus strains.

NA is a glycoside hydrolase enzyme (EC 3.2.1.18) that is found on the surface of the influenza virus and plays a pivotal role in the viral life cycle [7]. As such, NA cleaves the glycosidic bond of the terminal sialic acid from the host cell receptor with a new viral progeny release to infect other cells. Up to date, oseltamivir (Tamiflu®) and zanamivir (Relenza®), shown in Fig. 1, are the two common anti-influenza drugs targeted against, and operating as inhibitors of NA (NAIs). While oseltamivir is medicated as a tablet, zanamivir is administered by oral inhalation. Therefore, the oseltamivir is more commonly used to treat influenza patients. Another NAI drug, peramivir, was made available during the outbreak of the 2009 pandemic H1N1 virus until June 2010 under the Emergency Use Authorization (EUA) by the Food and Drug Administration (FDA)

* Corresponding author. Tel.: +66 22185426; fax: +66 22185418.
E-mail address: t.rungrotmongkol@gmail.com (T. Rungrotmongkol).
[1] These authors contributed equally to this work.

1093-3263/$ – see front matter © 2012 Elsevier Inc. All rights reserved.
http://dx.doi.org/10.1016/j.jmgm.2012.06.007

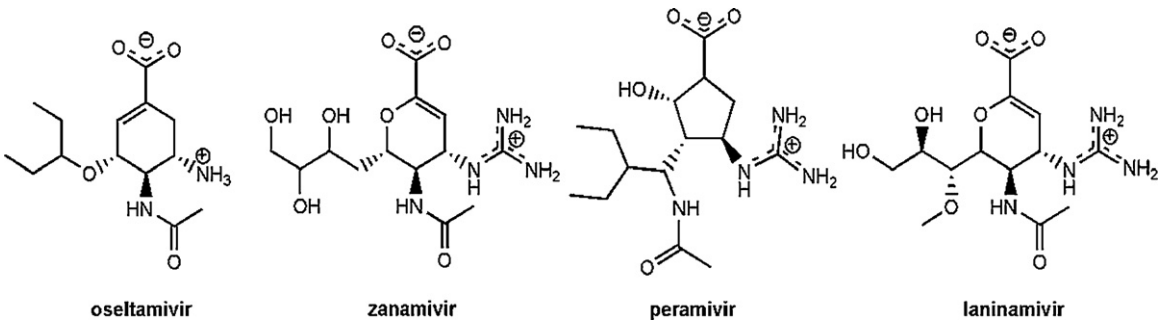

Fig. 1. The chemical structures of four NA inhibitors (NAIs) in the active metabolite form: oseltamivir, zanamivir, peramivir and laninamivir.

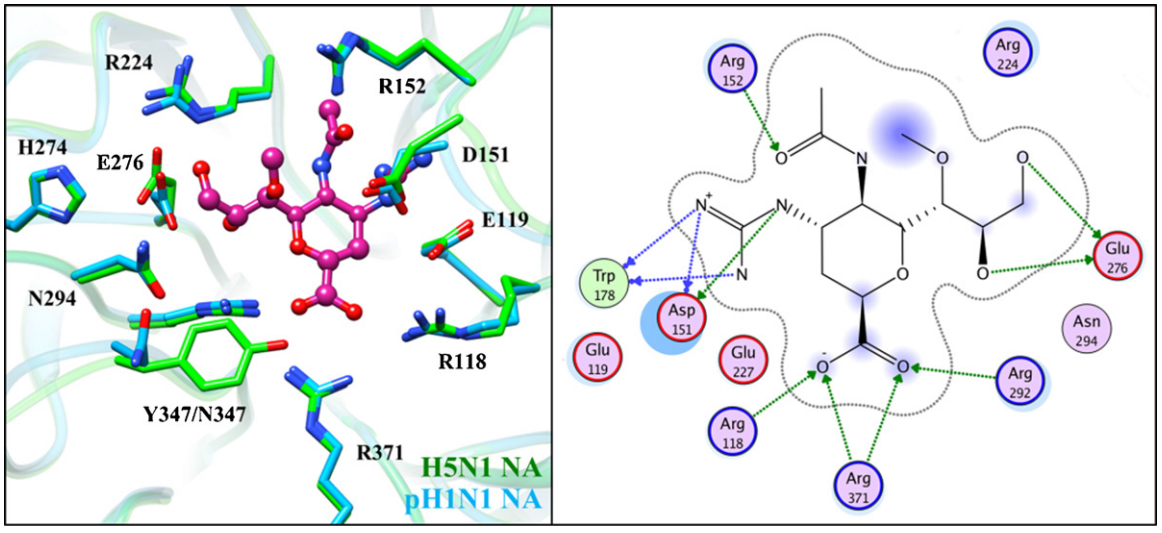

Fig. 2. (Left) Close up of laninamivir binding to the catalytic pocket of the pH1N1 NA (cyan) obtained from the 3TI3 crystal structure [6] with a superimposition of the H5N1 NA (2HU4 [15], green). (Right) From the X-ray structure of the laninamivir–NA complex, the hydrogen bond formations through the backbone and side chain of the surrounding residues are represented by blue and green arrows, respectively.

[8]. Recently, the second generation flu NAI drug, laninamivir, was discovered by Yamashita and co-workers [9] and manufactured by Daiichi Sankyo Co. Ltd. in Japan and Biota. It is an active metabolite converted in lung from the CS-8959 (laninamivir octanoate) prodrug [10,11]. Besides the long term efficient activity, with a single inhaled dose being comparable to that from taking oseltamivir twice daily for 5 days, laninamivir is effective against the wild-type strain of both influenza A (seasonal H1N1, pH1N1, H5N1 and H3N2) and B viruses as well as the oseltamivir-resistant H274Y mutations of H5N1, pH1N1 and seasonal H1N1 viruses [5,12,13] as summarized in Table 1. It is worth noting that the virus strain order, in terms of the fold increase in resistance to laninamivir, relative to wild-type is pH1N1 (1.36) < seasonal H1N1 (1.85) < H5N1 (3.44 or 7.50). In agreement with the experimental data, laninamivir and its prodrug were theoretically predicted to have high binding affinities with A/H5N1 complexes through the rupture forces and so that laninamivir could be used to inhibit both the WT and the oseltamivir-resistance providing N294S and H274Y mutations [14].

In order to understand the high susceptibility of NA from both the WT and H274Y mutant isolates of the influenza viruses towards the NAI laninamivir, molecular dynamics (MD) simulations were performed on the two influenza subtypes, H5N1 and pH1N1. The drug–target interactions, in terms of the hydrogen bonds, electrostatic and vdW forces, with the surrounding residues at the catalytic site of NA were intensively analyzed, discussed and compared with the co-crystal structure of pH1N1 NA with laninamivir bound, as well as with previous theoretical studies on the other anti-influenza NAI drugs.

2. Methodology

2.1. System preparation

All system preparations and MD simulations were performed using the AMBER10 software [16]. The four simulated systems of the WT and H274Y mutant of the NA from both the pH1N1 and H5N1 virus strains were prepared as follows. The starting structure of WT pH1N1 NA-inhibitor complex was taken from the recently determined co-crystal structure of the WT NA of pH1N1 virus with

Table 1
The 50% inhibitory concentration (IC_{50}) values of laninamivir for neuraminidase (NA) from various influenza strains.

Virus strain	NA change	IC_{50} (nM)	RF[b]
A/H1N1 (seasonal flu) [5]	WT	1.79	
pH1N1 [5]	WT	1.83	
A/H3N2 [5]	WT	2.13	
Influenza B [5]	WT	11–26	
A/Yogohama/67/2006 (seasonal H1N1) [13]	WT	3.03	
A/Yogohama/67/2006 (seasonal H1N1) [13]	H274Y	5.62	1.85
A/Washington/29/2009 (pH1N1) [12]	WT	1.57[a]	
A/Washington/29/2009 (pH1N1) [12]	H274Y	2.14[a]	1.36
A/Hanoi/30408/05 (HPAI H5N1) [13]	WT	0.32	
A/Hanoi/30408/05 (HPAI H5N1) [13]	H274Y	1.10	3.44
A/Vietnam/1203/04 (H5N1) [13]	WT	0.28	
A/Vietnam/1203/04 (H5N1) [13]	H274Y	2.10	7.50

[a] Fluorescein leakage (MUNANA) assay.
[b] RF = Resistance fold.

laninamivir bound (PDB entry code: 3TI3 [6]). To build the H274Y mutant system, the histidine at residue number 274 was changed to tyrosine from the refined crystal structure of apo pH1N1 NA (PDB code: 3NSS [17]). This procedure was done using the LEaP module implemented in AMBER10. The laninamivir was later added into the active site of the mutated H274Y pH1N1 NA. For the two laninamivir-H5N1 systems, the X-ray structures of the WT and H274Y forms of NA from H5N1 strains complexed with oseltamivir (PDB codes 2HU4 [15] and 3CL0 [1], respectively) were used where the atomic coordinates of oseltamivir were replaced by laninamivir. The Ca^{2+} and water molecules from the crystal structure were retained in the system. The ionizable amino acids, including K, R, D and E, were categorized at pH 7.0. The protonation state of histidine was assigned according to the identified hydrogen bond with the interacting partner. A possible disulfide bridge between two cysteines was assigned to maintain the protein stability. The missing hydrogen atoms of the NA protein and the laninamivir NAI in each system were added by the LEaP module.

The energy minimization with 2000 steps of steepest descent (SD) and continued by 1000 steps of conjugated gradient (CG) were initially performed on the hydrogen atoms to reduce bad steric contacts. Subsequently, each system was solvated by TIP3P waters [18], with a minimum distance of 12 Å from the protein surface. The water box size was 98 Å × 98 Å × 98 Å and 89 Å × 87 Å × 95 Å for the pH1N1 wild-type and H274Y, respectively, while those of H5N1 systems was 84 Å × 85 Å × 88 Å. The total negative charges were neutralized by adding Na^+ counterions. Afterwards, the crystal and modeled waters were minimized by 2000 steps of SD and 1000 steps of CG, and finally the whole system was optimized using the same procedure.

2.2. Partial charge and force field development for laninamivir

The partial atomic charges and empirical force field parameters of laninamivir were developed according to the standard scheme as in previous studies [19–22]. By considering the hybridization of the covalent bonds, the coordinates of the 22 missing hydrogen atoms were added to laninamivir structure. The ligand structure was optimized with the HF/6-31* basis set to adjust the bond lengths and bond angles using Gaussian 03 program [23]. To obtain electrostatic potential (ESP) surrounding ligand molecule, the single point calculation was performed at the same method and level of theory on the optimized geometry. Consequently, the restrained electrostatic potential (RESP) charges were evaluated with the charge-fitting procedure using the RESP module of AMBER program. The laninamivir parameters were derived from the generalized amber force field (GAFF) [24], while the standard van der Waals (vdW) parameters were utilized to adequate transferability of intermolecular interaction.

2.3. Molecular dynamics (MD) simulations

A single continuous MD simulation was applied on each of the four NA–laninamivir simulated complexes, being NA from the WT and H274Y mutation of both H5N1 and pH1N1 viral strains, where the periodic boundary with the NPT ensemble at 1 atm and a time step of 2 fs were employed. The whole system was heated up to 300 K for 50 ps and subsequently simulated at this temperature for 20 ns using the SANDER module in AMBER. The SHAKE algorithm was used to constrain all bonds involving hydrogen atoms [25]. The cutoff distance for non-bonded interactions was set at 12 Å and the particle mesh Ewald method [26] was applied to account for long-range electrostatic interactions. After the simulations were found to reach equilibrium, the MD trajectories were extracted from the production phase for analysis. The ptraj and MM-GBSA modules, as implemented in the AMBER software, were used to analyze the global root mean-square displacement (RMSD), hydrogen bond occupancy, decomposition of free energies per residue and their energy components, between laninamivir and each of the four targeted NA isoforms.

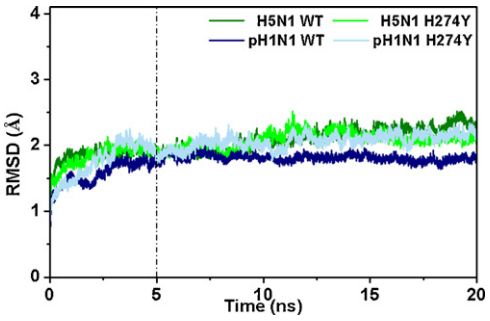

Fig. 3. Root mean-square displacements (RMSDs) relative to the starting structure for all atoms of the laninamivir binding to the WT and H274Y NAs of the influenza H5N1 and pH1N1 viruses.

3. Results and discussion

3.1. Stability of the global structure

To monitor the stability of the four studied systems, the RMSD values of all the atoms of the laninamivir NAI complexed to each of the four NAs (WT and H274Y NAs of the H5N1 and pH1N1 viruses) relative to the starting structure versus simulation time were measured and are shown in Fig. 3. As can be seen from the plot, the RMSD fluctuations are similar in three systems around 2.2 Å, excluding the pH1N1 WT shows lower fluctuation around 1.8 Å (after 3 ns). All complexes were likely to reach equilibrium at 5 ns. Therefore, the MD trajectories from the last 15 ns were extracted for all further analysis.

3.2. Laninamivir binding patterns

To understand the mechanism of action and drug–target interactions of the laninamivir binding to both the WT and H274Y mutation of both the H5N1 and pH1N1 NAs, hydrogen bonding interaction and the role of key acting residues on the basis of decomposition of binding free energy were investigated as follows.

3.2.1. Hydrogen bonding interactions

Since the active metabolite of laninamivir is a zwitterion with the $-COO^-$ and $-NHC(NH_2)_2^+$ groups, hydrogen bonding and salt bridge interactions play a critical role in stabilizing the protein–ligand complex. To gain further insight into the efficiency of the laninamivir binding to the NAs from the WT and H274Y mutation of the H5N1 and pH1N1 viruses, the percentage occupancy and the number of hydrogen bonds between this NAI and the surrounding NA residues were investigated according to the subsequent criteria: (i) the distance between proton donor (D) and acceptor (A) atoms was $\leq$3.5 Å; and (ii) the D–H···A angle was $\geq$120°. The hydrogen bond results and representative MD snapshots for the four complexes are depicted and compared in Fig. 4. Strong and moderate hydrogen bonding interactions are defined as having hydrogen bond occupations of >75% and 50–75%, respectively.

As can be seen in Fig. 4, the major hydrogen bonding interactions between the laninamivir and the NA binding residues are almost similar among all four NA–laninamivir complexes, although they are slightly different at some amino acids. Even though the Y347 of H5N1 is replaced by N347 in pH1N1, the NA–laninamivir interaction still slightly changes. Differentially, the interaction between pH1N1 NA and oseltamivir was weakened due to the outwardly

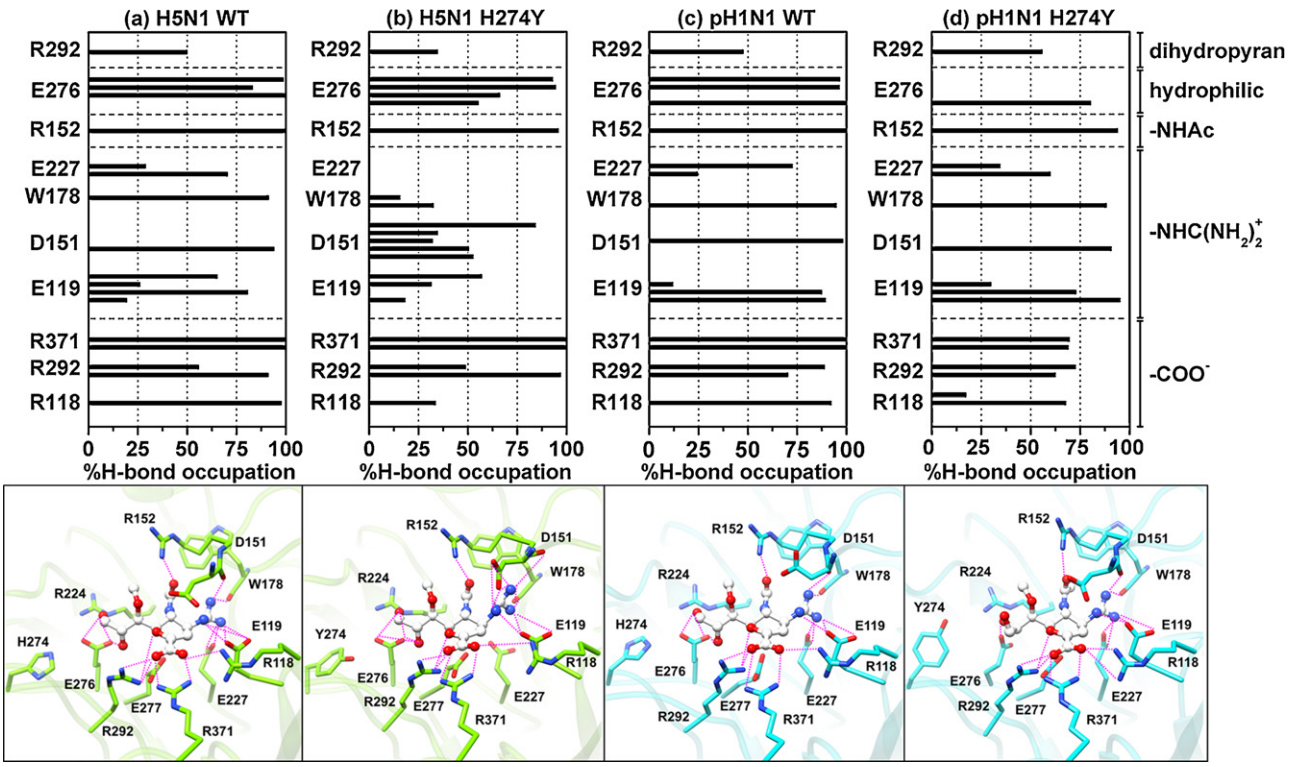

Fig. 4. Percent occupation pattern of hydrogen bonds formed from the dihydropyran ring and the four side chains of laninamivir to the binding residues (label given along *y*-axis) in the active site of the four NAs: (a) H5N1 WT, (b) H5N1 H274Y, (c) pH1N1 WT and (d) pH1N1 H274Y.

oriented N347 from the binding site which decreased the average number of hydrogen bonds over simulation time with a presence of the wider pocket as noticed in the previous theoretical study [27]. The ether oxygen of the dihydropyran ring and the carbonyl oxygen of the –NHAc moiety established moderate and strong hydrogen bonding interactions with the nitrogen atoms of the guanidinium of NA residues R292 and R152, respectively. Interestingly, the former hydrogen bond with R292 was only observed in the laninamivir complexes of both strains. This phenomenon is not always found in zanamivir complexes, where the moderate hydrogen bond formation with dihydropyran scaffold was detected in pH1N1 NA, but not in H5N1 NA [27]. Meanwhile the latter one with R152 is typically detected in the other anti-influenza NA drugs and potent compounds [19,28–33]. In contrast to that for laninamivir–NA seen here, the H274Y mutation of NA was observed to disrupt the hydrogen bond of oseltamivir with the NA R152 residue [31,34,35], thereby probably resulting in the low drug inhibitory potency of oseltamivir. In contrast, this strong interaction with R152 and laninamivir could possibly account for the high NAI activity of laninamivir against the oseltamivir-resistant H274Y mutation. From the electrostatic surface study of oseltamivir binding pathway [35], the mutated residue 274 positioned directly onto the negatively charged funnel at the mouth of the binding pocket has perhaps caused a different electrostatic drug–target interaction. Moreover, the Y274 replacement significantly reduced the hydrophobic pocket size for the oseltamivir's bulky group as seen by an increase of solvent accessible surface area (SASA), instead of disrupting E276–R224 salt bridge [2,34].

However, some noticeable differences between the four H-bond patterns were detected at the 2,3-dihydroxy-1-methoxypropyl (hydrophilic bulky), $-NHC(NH_2)_2^+$ and $-COO^-$ moieties of the laninamivir ligand. The strong interaction strength between the hydrophilic bulky group of laninamivir and the E276 residue of NA was likely maintained in all complexes, although the percentage and number of hydrogen bonds were different. Stronger and larger numbers of hydrogen bond formations were observed in the case of the WT NA of both viruses and for the H5N1 H274Y mutant, while only one strong interaction was observed in the case of the H274Y NA from pH1N1. Conversely, the replacement of the hydrophilic group by hydrophobic side chain such as in oseltamivir or peramivir usually brings a loss of hydrogen bond formation with NA [5,15,36,37]. The change to a methoxy group at this hydrophilic side chain, instead of all three hydroxyl groups in zanamivir, led to no interaction with NA residue R224 in the H5N1 WT [19] and N294 (N2 numbering) in the pH1N1 WT [29].

At the $-NHC(NH_2)_2^+$ group, the positively charged side chain was well stabilized by the three negatively charged residues, E119, D151 and E227, as well as the W178 backbone (Fig. 4, and discussed below), similar to that which was observed in the previous studies on the zanamivir– and peramivir–NA systems [28,29,31]. This part of the laninamivir formed a rather strong salt bridge interaction with NA residue E119 in the case of WT strains for H274Y mutant. A strong interaction with NA residue D151 was conserved in all four complexes although that with the H5N1 H274Y form of NA provided a larger number of weak and moderate salt bridge interactions than the other three NA–laninamivir systems. With almost 100% occupation of this laninamivir–NA interaction in the H5N1 WT and the two pH1N1 strains, one can imply that in complex with laninamivir the 150-loop of NA eventually and tightly moved to lock the inhibitor. Again, the guanidinium nitrogen of laninamivir created a strong hydrogen bond with the backbone carbonyl oxygen of NA residue W178 in all strains except the H274Y mutant of H5N1 complex which showed weaken interaction. This observation is different from those of oseltamivir binding to the WT and H274Y NA mutant of both H5N1 and pH1N1, where the hydrogen bond to W178 was completely lost [31,34,38], with a consequence of an increased resistance to this NAI in comparison to that for laninamivir. In addition, moderate hydrogen bonding between laninamivir and NA residue E227 was detected in H5N1 WT and two of pH1N1, but this was totally lost in the case of H5N1

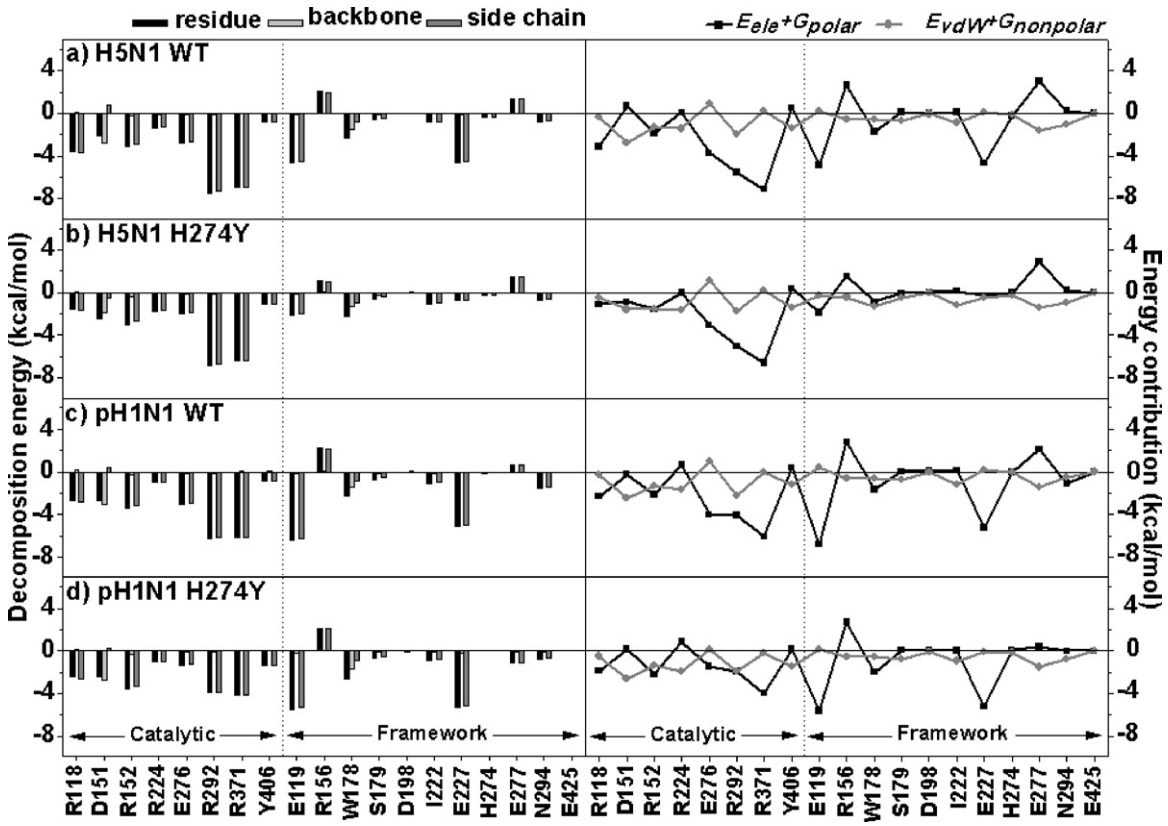

Fig. 5. The (left) decomposition of the binding free energy in pairwise per-residue basis ($\Delta G_{bind}^{residue}$), and its energy contributions from the backbone ($\Delta G_{bind}^{backbone}$) and side chain ($\Delta G_{bind}^{sidechain}$) atoms, and (right) the electrostatic ($E_{ele}+G_{polar}$) and vdW ($E_{vdW}+G_{nonpolar}$) energy.

H274Y. It should be mentioned that the replacement of $-(NH_3)^+$ in oseltamivir by the longer $-NHC(NH_2)_2^+$ group in laninamivir (also in zanamivir) introduced the interaction with the NA residue E227.

As expected, the three conserved arginines of NA, R118, R292 and R371, were found to contribute extensively through salt bridge interactions to stabilize the $-COO^-$ moiety of laninamivir in the two WT NA strains. These important drug–target interactions are commonly detected in all NAIs and drug candidates containing a negatively charged group [19,32,39–41]. Interestingly, the H274Y mutation has been found to interrupt the drug–target interactions with R118 (to 34% occupation) in H5N1 NA and partially disturb the arginine triad (to ~70%) in pH1N1 NA. The interaction with R118 was dramatically reduced from ~90% in the oseltamivir–NA (WT) complex of the pH1N1 to ~5% in the oseltamivir–NA (H274Y) complex [38].

3.2.2. Key residues for drug binding

To pinpoint the important residues for the binding of laninamivir in the NA active site of influenza H5N1 and H1N1 viruses, the interaction energy from the individual residues of NA that contributed to laninamivir binding were evaluated according to the MM-GBSA method [42–44] using the decomposition energy module of AMBER. Note that the measured residues are comprised of the eight catalytic residues (R118, D151, R152, R224, E276, R292, R371 and Y406) and the 11 framework residues (E119, R156, W178, S179, D198, I222, E227, H274, E277, N294 and E425). The binding free energy decomposition as a pairwise per-residue basis ($\Delta G_{bind}^{residue}$), and the contribution separated into the residue backbone ($\Delta G_{bind}^{backbone}$) and the side chain ($\Delta G_{bind}^{sidechain}$), are plotted in Fig. 5 (left), whereas the corresponding electrostatic ($E_{ele}+G_{polar}$) and vdW ($E_{vdW}+G_{nonpolar}$) energy terms are shown in Fig. 5 (right).

Almost all the NA residues (except for D151 and W178) provided some energy stabilizations towards laninamivir through their side chains, in correspondence with the observed presence of drug–target hydrogen bonds. Among the NA residues in the WT strain of the two viruses (Fig. 5a and c, left), the highest contribution was likely gained from the laninamivir contacting NA residues through a strong salt-bridge (in terms of electrostatic energy in Fig. 5, right) and hydrogen bond interactions with the charged groups of laninamivir (mentioned above). These are the R292 and R371 residues in the catalytic site and the E119 (pH1N1) residue in the framework site with $\Delta G_{bind}^{residue}$ of less than -6 kcal/mol. Additionally, the residues R118, E119 (H5N1), D151, R152, W178, E227 and E276 gave an energy contribution in the range of $-2 \leq \Delta G_{bind}^{residue} \leq -6$ kcal/mol. Although most NA residues preferentially stabilized the laninamivir binding to NA, destabilization can be found at the framework residues R156 and E277. Contrary to the oseltamivir complex, the R118 residue plays the role to disrupt the binding stability between oseltamivir and receptor by ~2 kcal/mol of energy contribution as reported in the previous work [45].

In the H274Y NA mutation, the laninamivir–NA interactions were apparently reduced to at least half-strength for H5N1 at the catalytic residue R118 and at the framework residues E119 and E227 (Fig. 5b, left), in accord with the observed decrease in the number and/or occupation of predicted hydrogen bonds (Fig. 5b). In some similar features, the situation is different for the pH1N1 H274Y NA mutant, in which the energy reduction was primarily found at the catalytic residue E276 (by ~−2 kcal/mol) and a lowered interaction at the two conserved arginines R292 and R371 (energy increased to ~−4 kcal/mol).

Taking into account the hydrogen bonding and per-residue binding free energy decomposition, the laninamivir–NA

interactions were somewhat lowered in the H274Y NA isoform relative to that of the WT form in both the H5N1 and pH1N1 viruses. This is in good agreement with the experimental evidence that shows slightly increased IC_{50} values, i.e., 1.36-fold resistance for pH1N1 [12], and 3.4- and 7.5-fold resistance for H5N1 [13] compared to the WT (Table 1). However, most contributions to the laninamivir–NA were largely conserved. This information could support the high inhibitory potency of laninamivir against not only the wild-type NA strain but also the H274Y mutant of the viral influenza subtypes H5N1 and H1N1.

4. Conclusions

MD simulations were applied to investigate the susceptibility of the WT and H274Y mutant isoforms of NA from the influenza A virus subtypes H5N1 and pH1N1 towards the NAI laninamivir, in terms of the structure and dynamic properties, drug–target interactions and binding pattern. The results show all the important interactions of laninamivir with NA are conserved. Indeed, even when histidine at the 274 position was transformed to tyrosine only slightly decreased interaction strength at some residues was observed (R118, W178 and R152). In comparison to oseltamivir, the laninamivir guanidinium and hydrophilic side chains are indispensable to lock the two framework residues (W178 and E227) and a catalytic residue (E276), respectively, better than those groups of oseltamivir at the relative positions. Most positive contributions to the interaction were found from the side chains of 7 of the catalytic NA residues (R118, D151, R152, R224, E276, R292 and R371), and 4 of the framework residues (E119, W178, E227 and E277), through electrostatic interactions and in particular salt bridge interactions and hydrogen bond formation. In contrast, in the case of oseltamivir (the most widely used NAI anti-influenza drug), the important drug–target interactions were dramatically reduced and totally lost in the H274Y NA isoforms from the H5N1 and pH1N1 viral strains with a result of a high-level of resistance to oseltamivir. For the example, the oseltamivir interaction with W178 and R152 was significantly dwindled. This is, therefore, the likely explanation for the high susceptibility of both the WT and H274Y strains of H5N1 and pH1N1 viruses to laninamivir, in contrast to oseltamivir. However, it must be noted that only a single simulation was performed for each system, so the stability and preponderance of the interactions were unable to extrapolate conclusively. Based on overall data gained from the present study, the simulated results suggested that the drug hydrophilic moieties, $-COO^-$ and $-NHC(NH_2)_2^+$, are necessary for strong hydrogen bonding formation with NA, therefore modification on these groups may bring to a more powerful anti-influenza drugs. The replacement of the $-COO^-$ group by more negatively charged group such as phosphate or sulfonate possibly leads to higher interaction with the conserved arginine triad, while the positively charged group might be lengthened in order to increase in drug–target interaction for the open 150-loop conformation of NA.

Acknowledgments

This work was supported by the Asia Research Center, Chulalongkorn University. A.M. thanks the Royal Golden Jubilee Ph.D. Program (PHD/0271/2549). We further thank the Thailand Research Fund, Thailand Research Fund (DPG5480002), the National Research University Project of Thailand, Office of the Higher Education Commission (HR1155A-55), and the Thai Government Stimulus Package 2 (TKK2555) under the Project for Establishment of Comprehensive Center for Innovative Food, Health Products and Agriculture. The Center of Excellence for Petroleum, Petrochemicals and Advanced Materials, Chulalongkorn University, is acknowledged.

References

[1] P.J. Collins, L.F. Haire, Y.P. Lin, J. Liu, R.J. Russell, P.A. Walker, J.J. Skehel, S.R. Martin, A.J. Hay, S.J. Gamblin, Crystal structures of oseltamivir-resistant influenza virus neuraminidase mutants, Nature 453 (2008) 1258–1261.
[2] G. Neumann, T. Noda, Y. Kawaoka, Emergence and pandemic potential of swine-origin H1N1 influenza virus, Nature 459 (2009) 931–939.
[3] M. Yamashita, T. Tomozawa, M. Kakuta, A. Tokumitsu, H. Nasu, S. Kubo, CS-8958, a prodrug of the new neuraminidase inhibitor R-125489, shows long-acting anti-influenza virus activity, Antimicrobial Agents and Chemotherapy 53 (2009) 186–192.
[4] S. Kubo, T. Tomozawa, M. Kakuta, A. Tokumitsu, M. Yamashita, Laninamivir prodrug CS-8958, a long-acting neuraminidase inhibitor, shows superior anti-influenza virus activity after a single administration, Antimicrobial Agents and Chemotherapy 54 (2010) 1256–1264.
[5] N. Sugaya, Y. Ohashi, Long-acting neuraminidase inhibitor laninamivir octanoate (CS-8958) versus oseltamivir as treatment for children with influenza virus infection, Antimicrobial Agents and Chemotherapy 54 (2010) 2575–2582.
[6] C.J. Vavricka, Q. Li, Y. Wu, J. Qi, M. Wang, Y. Liu, F. Gao, J. Liu, E. Feng, J. He, J. Wang, H. Liu, H. Jiang, G.F. Gao, Structural and functional analysis of laninamivir and its octanoate prodrug reveals group specific mechanisms for influenza NA inhibition, PLoS Pathogens 7 (2011) e1002249.
[7] T. Rungrotmongkol, P. Yotmanee, N. Nunthaboot, S. Hannongbua, Computational studies of influenza A virus at three important targets: hemagglutinin, neuraminidase and M2 protein, Current Pharmaceutical Design 17 (2011) 1720–1739.
[8] D. Birnkrant, E. Cox, The emergency use authorization of peramivir for treatment of 2009 H1N1 influenza, New England Journal of Medicine 361 (2009) 2204–2207.
[9] T. Honda, T. Masuda, S. Yoshida, M. Arai, S. Kaneko, M. Yamashita, Synthesis and anti-influenza virus activity of 7-O-alkylated derivatives related to zanamivir, Bioorganic and Medicinal Chemistry Letters 12 (2002) 1925–1928.
[10] K. Koyama, M. Takahashi, M. Oitate, N. Nakai, H. Takakusa, S.-i. Miura, O. Okazaki, CS-8958, a prodrug of the novel neuraminidase inhibitor R-125489, demonstrates a favorable long-retention profile in the mouse respiratory tract, Antimicrobial Agents and Chemotherapy 53 (2009) 4845–4851.
[11] Y. Makoto, R-118958, a unique anti-influenza agent showing high efficacy for both prophylaxis and treatment after a single administration: from the in vitro stage to phase I study, International Congress Series 1263 (2004) 38–42.
[12] H.T. Nguyen, T.G. Sheu, V.P. Mishin, A.I. Klimov, L.V. Gubareva, Assessment of pandemic and seasonal influenza A (H1N1) virus susceptibility to neuraminidase inhibitors in three enzyme activity inhibition assays, Antimicrobial Agents and Chemotherapy 54 (2010) 3671–3677.
[13] M. Yamashita, Laninamivir its prodrug CS-8958: long-acting neuraminidase inhibitors for the treatment of influenza, Antiviral Chemistry and Chemotherapy 21 (2010) 71–84.
[14] B.K. Mai, M.S. Li, Neuraminidase inhibitor R-125489 – a promising drug for treating influenza virus: steered molecular dynamics approach, Biochemical and Biophysical Research Communications 410 (2011) 688–691.
[15] R.J. Russell, L.F. Haire, D.J. Stevens, P.J. Collins, Y.P. Lin, G.M. Blackburn, A.J. Hay, S.J. Gamblin, J.J. Skehel, The structure of H5N1 avian influenza neuraminidase suggests new opportunities for drug design, Nature 443 (2006) 45–49.
[16] D.A. Case, T.A. Darden, T.E.I. Cheatham, C.L. Simmerling, J. Wang, R.E. Duke, R. Luo, W. Crowley, R.C. Walker, W. Zhang, K.M. Merz, B. Wang, S. Hayik, A. Roitberg, G. Seabra, I. Kolossváry, K.F. Wong, F. Paesani, J. Vanicek, X. Wu, S.R. Brozell, T. Steinbrecher, H. Gohlke, L. Yang, C. Tan, J. Mongan, V. Hornak, G. Cui, D.H. Mathews, M.G. Seein, C. Sagui, V. Babin, P.A. Kollman, AMBER 10, 2008.
[17] Q. Li, J. Qi, W. Zhang, C.J. Vavricka, Y. Shi, J. Wei, E. Feng, J. Shen, J. Chen, D. Liu, J. He, J. Yan, H. Liu, H. Jiang, M. Teng, X. Li, G.F. Gao, The 2009 pandemic H1N1 neuraminidase N1 lacks the 150-cavity in its active site, Nature Structural & Molecular Biology 17 (2010) 1266–1268.
[18] W. Jorgensen, J. Chandrasekhar, J. Madura, R. Impey, M. Klein, Comparison of simple potential functions for simulating liquid water, Journal of Chemical Physics 79 (1983) 926–935.
[19] T. Udommaneethanakit, T. Rungrotmongkol, U. Bren, V. Frecer, M. Stanislav, Dynamic behavior of avian influenza A virus neuraminidase subtype H5N1 in complex with oseltamivir, zanamivir, peramivir, and their phosphonate analogues, Journal of Chemical Information and Modeling 49 (2009) 2323–2332.
[20] U. Arsawang, O. Saengsawang, T. Rungrotmongkol, P. Sornmee, K. Wittayanarakul, T. Remsungnen, S. Hannongbua, How do carbon nanotubes serve as carriers for gemcitabine transport in a drug delivery system? Journal of Molecular Graphics and Modelling 29 (2011) 591–596.
[21] W. Khuntawee, T. Rungrotmongkol, S. Hannongbua, Molecular dynamic behavior and binding affinity of flavonoid analogues to the cyclin dependent kinase 6/cyclin D complex, Journal of Chemical Information and Modeling 52 (2012) 76–83.
[22] P. Sornmee, T. Rungrotmongkol, O. Saengsawang, U. Arsawang, T. Remsungnen, S. Hannongbua, Understanding the molecular properties of doxorubicin filling inside and wrapping outside single-walled carbon nanotubes, Journal of Computational and Theoretical Nanoscience 8 (2011) 1385–1391.

[23] M.J. Frisch, G.W. Trucks, H.B. Schlegel, G.E. Scuseria, M.A. Robb, J.R. Cheeseman, J.A. Montgomery Jr., T. Vreven, K.N. Kudin, J.C. Burant, J.M. Millam, S.S. Iyengar, J. Tomasi, V. Barone, B. Mennucci, M. Cossi, G. Scalmani, N. Rega, G.A. Petersson, H. Nakatsuji, M. Hada, M. Ehara, K. Toyota, R. Fukuda, J. Hasegawa, M. Ishida, T. Nakajima, Y. Honda, O. Kitao, H. Nakai, M. Klene, X. Li, J.E. Knox, H.P. Hratchian, J.B. Cross, V. Bakken, C. Adamo, J. Jaramillo, R. Gomperts, R.E. Stratmann, O. Yazyev, A.J. Austin, R. Cammi, C. Pomelli, J.W. Ochterski, P.Y. Ayala, K. Morokuma, G.A. Voth, P. Salvador, J.J. Dannenberg, V.G. Zakrzewski, S. Dapprich, A.D. Daniels, M.C. Strain, O. Farkas, D.K. Malick, A.D. Rabuck, K. Raghavachari, J.B. Foresman, J.V. Ortiz, Q. Cui, A.G. Baboul, S. Clifford, J. Cioslowski, B.B. Stefanov, G. Liu, A. Liashenko, P. Piskorz, I. Komaromi, R.L. Martin, D.J. Fox, T. Keith, M.A. Al-Laham, C.Y. Peng, A. Nanayakkara, M. Challacombe, P.M.W. Gill, B. Johnson, W. Chen, M.W. Wong, C. Gonzalez, J.A. Pople, Gaussian 03, Revision C.02, Gaussian, Inc., Wallingford, CT, 2004.
[24] J. Wang, R.M. Wolf, J.W. Caldwell, P.A. Kollman, D.A. Case, Development and testing of a general amber force field, Journal of Computational Chemistry 25 (2004) 1157–1174.
[25] J.P. Ryckaert, G. Ciccotti, H.J.C. Berendsen, Numerical integration of the cartesian equations of motion of a system with constraints: molecular dynamics of n-alkanes, Journal of Computational Physics 23 (1977) 327–341.
[26] D.M. York, T.A. Darden, L.G. Pedersen, The effect of long-range electrostatic interactions in simulations of macromolecular crystals: a comparison of the Ewald and truncated list methods, Journal of Chemical Physics 99 (1993) 8345–8348.
[27] B.K. Mai, M.H. Viet, M.S. Li, Top leads for swine influenza A/H1N1 virus revealed by steered molecular dynamics approach, Journal of Chemical Information and Modeling 50 (2010) 2236–2247.
[28] M. Malaisree, T. Rungrotmongkol, P. Decha, P. Intharathep, O. Aruksakunwong, S. Hannongbua, Understanding of known drug–target interactions in the catalytic pocket of neuraminidase subtype N1, Proteins: Structure, Function, and Bioinformatics 71 (2008) 1908–1918.
[29] D. Pan, H. Sun, C. Bai, Y. Shen, N. Jin, H. Liu, X. Yao, Prediction of zanamivir efficiency over the possible 2009 influenza A (H1N1) mutants by multiple molecular dynamics simulations and free energy calculations, Journal of Molecular Modeling 17 (2011) 2465–2473.
[30] T. Rungrotmongkol, P. Intharathep, M. Malaisree, N. Nunthaboot, N. Kaiyawet, P. Sompornpisut, S. Payungporn, Y. Poovorawan, S. Hannongbua, Susceptibility of antiviral drugs against 2009 influenza A (H1N1) virus, Biochemical and Biophysical Research Communications 385 (3) (2009) 390–394.
[31] L. Le, E. Lee, K. Schulten, T.N. Truong, Molecular modeling of swine influenza A/H1N1 Spanish H1N1, and avian H5N1 flu N1 neuraminidases bound to Tamiflu and Relenza, PLoS Currents 1 (2009) RRN1015.
[32] P. Bonnet, R.A. Bryce, Molecular dynamics and free energy analysis of neuraminidase–ligand interactions, Protein Science 13 (2004) 946–957.
[33] D.-Q. Wei, Q.-S. Du, H. Sun, K.-C. Chou, Insights from modeling the 3D structure of H5N1 influenza virus neuraminidase and its binding interactions with ligands, Biochemical and Biophysical Research Communications 344 (3) (2006) 1048–1055.
[34] M. Malaisree, T. Rungrotmongkol, N. Nunthaboot, O. Aruksakunwong, P. Intharathep, P. Decha, P. Sompornpisut, S. Hannongbua, Source of oseltamivir resistance in avian influenza H5N1 virus with the H274Y mutation, Amino Acids 37 (2009) 725–732.
[35] L. Le, E.H. Lee, D.J. Hardy, T.N. Truong, K. Schulten, Molecular dynamics simulations suggest that electrostatic funnel directs binding of Tamiflu to influenza N1 neuraminidases, PLoS Computational Biology 6 (2010) e1000939.
[36] A.J. Oakley, S. Barrett, T.S. Peat, J. Newman, V.A. Streltsov, L. Waddington, T. Saito, M. Tashiro, J.L. McKimm-Breschkin, Structural and functional basis of resistance to neuraminidase inhibitors of influenza B viruses, Journal of Medicinal Chemistry 53 (2010) 6421–6431.
[37] J.N. Varghese, P.W. Smith, S.L. Sollis, T.J. Blick, A. Sahasrabudhe, J.L. McKimm-Breschkin, P.M. Colman, Drug design against a shifting target: a structural basis for resistance to inhibitors in a variant of influenza virus neuraminidase, Structure (London, England: 1993) 6 (1998) 735–746.
[38] T. Rungrotmongkol, M. Malaisree, N. Nunthaboot, P. Sompornpisut, S. Hannongbua, Molecular prediction of oseltamivir efficiency against probable influenza A (H1N1-2009) mutants: molecular modeling approach, Amino Acids 39 (2010) 393–398.
[39] T. Rungrotmongkol, V. Frecer, W. De-Eknamkul, S. Hannongbua, S. Miertus, Design of oseltamivir analogs inhibiting neuraminidase of avian influenza virus H5N1, Antiviral Research 82 (2009) 51–58.
[40] J.J. Shie, J.M. Fang, S.Y. Wang, K.C. Tsai, Y.S. Cheng, A.S. Yang, S.C. Hsiao, C.Y. Su, C.H. Wong, Synthesis of Tamiflu and its phosphonate congeners possessing potent anti-influenza activity, Journal of the American Chemical Society 129 (2007) 11892–11893.
[41] T. Rungrotmongkol, T. Udommaneethanakit, V. Frecer, S. Miertus, Combinatorial design of avian influenza neuraminidase inhibitors containing pyrrolidine core with a reduced susceptibility to viral drug resistance, Combinatorial Chemistry & High Throughput Screening 13 (2010) 268–277.
[42] H. Gohlke, C. Kiel, D.A. Case, Insights into protein–protein binding by binding free energy calculation and free energy decomposition for the Ras–Raf and Ras–RalGDS complexes, Journal of Molecular Biology 330 (2003) 891–913.
[43] T. Rungrotmongkol, N. Nunthaboot, M. Malaisree, N. Kaiyawet, P. Yotmanee, A. Meeprasert, S. Hannongbua, Molecular insight into the specific binding of ADP-ribose to the nsP3 macro domains of chikungunya and Venezuelan equine encephalitis viruses: molecular dynamics simulations and free energy calculations, Journal of Molecular Graphics and Modelling 29 (2010) 347–353.
[44] V. Zoete, M. Meuwly, M. Karplus, Study of the insulin dimerization: binding free energy calculations and per-residue free energy decomposition, Proteins: Structure, Function, and Bioinformatics 61 (2005) 79–93.
[45] H. Liu, X. Yao, C. Wang, J. Han, In silico identification of the potential drug resistance sites over 2009 influenza A (H1N1) virus neuraminidase, Molecular Pharmacology 7 (2010) 894–904.